

Syntheses, Crystal Structures, and Gas Storage Studies in New Three-Dimensional 5-Aminoisophthalate Praseodymium Polymeric Complexes

Yongcai Qiu,^{†,‡} Hong Deng,^{*,†} Shihe Yang,[‡] Jixia Mou,[†] Carole Daiguebonne,^{||} Nicolas Kerbellec,^{||} Olivier Guillou,^{*,||} and Stuart R. Batten[⊥]

School of Chemistry & Environment and Key Laboratory of Electrochemical Technology on Energy Storage and Power Generation in Guangdong Universities, South China Normal University, Guangzhou 510006, China, Nano Science and Technology Program, Department of Chemistry, The Hong Kong University of Science and Technology, Clear Water Bay, Kowloon, Hong Kong, Université Européenne de Bretagne-UMR CNRS-INSA 6226, Sciences Chimiques de Rennes, 20 Avenue des buttes de Coësmes, 35043 Rennes, France, and School of Chemistry, Monash University, Victoria 3800, Australia

Received October 26, 2008

The hydrothermal reaction of 5-aminoisophthalic acid and praseodymium oxide in different acids results in two new praseodymium coordination polymers, $\{\text{Pr}_2(\text{aip})_3(\text{H}_2\text{O})_2 \cdot 3\text{H}_2\text{O}\}_n$ (**1**) and $\{\text{Pr}_2(\text{Haip})_2(\text{aip})(\text{NO}_3)_2 \cdot 8\text{H}_2\text{O}\}_n$ (**2**) (aip = 5-aminoisophthalate). Complexes **1** and **2** are two distinct three-dimensional metal-organic frameworks constructed from the linkage of rod-shaped praseodymium carboxylate secondary building units and phenyl rings. Both dehydrated coordination frameworks are estimated using a computational method based on Connolly's algorithm, indicating that dehydrated compound **1** cannot host molecules other than water molecules or He, whereas dehydrated compound **2** is able to host molecules with kinetic radii as big as 2.3 Å. The potential specific accessible surface of this compound is 792 m² g⁻¹. Meanwhile, N₂ sorption measurements reveal that dehydrated compound **2** having a high 230 cm³/g (287 mg/g) N₂ storage capacity at 77 K and 1 atm is in fairly good agreement with our calculation results. Moreover, powder X-ray diffraction measurement results demonstrated that the stable channels of dehydrated compound **2** can reversibly host other small solvent molecules (e.g., water, methanol, and ethanol) and grand canonical Monte Carlo simulation is applied to predict its hydrogen storage capacity.

Introduction

There is currently a great deal of interest in the design and construction of 3-D metal-organic frameworks (MOFs) created by joining the metal ions with organic linkers because of their intriguing structural topologies and their versatile applications in the areas of redox catalysis, ion exchange, adsorption, separation, sensors, and photoluminescence.^{1–6} A number of porous materials constructed by the assembly of discrete metal-carboxylate clusters and organic linkers have been shown to be amenable to tuning of the size and

surface properties of the pores.⁷ For example, a systematic study of MOF-5 and its analogues was exemplified in a report by Yaghi and co-workers, where the metal-carboxylate Zn₄O(COO)₄ octahedral clusters as secondary building units (SBUs) are interconnected by aromatic rings of different lengths.^{7a} Other discrete SBU shapes (triangles, squares, tetrahedra, etc.) have also been used to synthesize other MOFs with useful physical–chemical properties and intriguing structural topologies.⁸

* To whom correspondence should be addressed. E-mail: dh@scun.edu.cn.

[†] South China Normal University.

[‡] Nano Science and Technology Program, Department of Chemistry, The Hong Kong University of Science and Technology.

^{||} Université Européenne de Bretagne.

[⊥] Monash University.

(1) Review articles: (a) Stang, P. J.; Olenyuk, B. *Acc. Chem. Res.* **1997**, *30*, 502. (b) Batten, S.; Robson, R. *Angew. Chem., Int. Ed.* **1998**, *37*, 1460. (c) Cheetham, A. K.; Ferey, G.; Loiseau, T. *Angew. Chem., Int. Ed.* **1999**, *38*, 3268. (d) Eddaoudi, M.; Moler, D. B.; Li, H. L.; Chen, B. L.; Reineke, T. M.; O'Keeffe, M.; Yaghi, O. M. *Acc. Chem. Res.* **2001**, *34*, 319. (e) Janiak, C. *Dalton Trans.* **2003**, 2781. (f) Bradshaw, D.; Claridge, J. B.; Cussen, E. J.; Prior, T. J.; Rosseinsky, M. J. *Acc. Chem. Res.* **2005**, *38*, 273. (g) Ferey, G.; Mellot-Draznieks, C.; Serre, C.; Millange, F. *Acc. Chem. Res.* **2005**, *38*, 217.

Recently, MOFs based on infinite rod-shaped SBUs have been extensively used to construct transition-metal-organic frameworks which do not interpenetrate due to the intrinsic arrangement of these rods in the structural assembly;⁹ however, lanthanide metal compounds have received less attention.¹⁰ The lanthanide ions have a strong tendency to adopt high coordination numbers, and their variable and versatile coordination behavior makes the design of porous coordination frameworks difficult.¹¹

A significant body of work on the construction of coordination polymers based on the 5-aminoisophthalate ligand (aip) has already been reported, but this work has focused mainly on transition metal ions.¹² Lanthanide metal ions have a strong preference to bind to carboxyl O-donor atoms, and the free amino group has a potential ability to form H bonds with solvent molecules. Thus, the 5-aminoisophthalate ligand may be effective in constructing porous lanthanide metal-organic frameworks.

In this paper, we highlight hydrothermal synthesis as a powerful method for the preparation of coordination polymers and isolate two new porous praseodymium coordination polymers $\{\text{Pr}_2(\text{aip})_3(\text{H}_2\text{O})_2 \cdot 3\text{H}_2\text{O}\}_n$ (**1**) and $\{\text{Pr}_2(\text{Haip})_2(\text{aip})(\text{NO}_3)_2 \cdot 8\text{H}_2\text{O}\}_n$ (**2**), which have been characterized by IR spectroscopy, elemental analysis, thermogravimetric analysis (TGA), power X-ray diffraction, and single-crystal diffraction. In particular, the potential porosities of the dehydrated coordination polymers were estimated using a computational method based on Connolly's algorithm. Moreover, N₂ sorption measurements and grand canonical Monte Carlo simulation (GCMC) reveal that dehydrated compound **2** exhibits reversible type I isotherm behavior indicative of a microporous material and nice hydrogen storage capacity, respectively.

Experimental Section

General Remarks. All materials and reagents were obtained commercially and were used without further purification. Elemental (C, H, N) analyses were performed on a Perkin-Elmer 2400 element analyzer. Infrared samples were prepared as KBr pellets, and spectra were obtained in the 400~4000 cm⁻¹ range using a Nicolet Avatar 360 FT-IR spectrophotometer. TGA experiments were performed on a NETZSCH TG 209 instrument with a heating rate of 10 °C min⁻¹. Powder XRD investigations were carried out on a Bruker AXS D8-Advanced diffractometer at 40 kV and 40 mA with Cu K α ($\lambda = 1.5406 \text{ \AA}$) radiation.

Preparation of Compound 1. A mixture of 5-aminoisophthalic acid (0.181 g, 1 mmol), Pr₆O₁₁ (0.150 g, 0.147 mmol), HClO₄ (1.90 mmol), and H₂O (10 mL) was heated to 150 °C for 50 h in a 23 mL Teflon-lined stainless-steel autoclave, and then it was cooled to room temperature at 10 °C h⁻¹ to obtain colorless block single crystals of **1** (yield: 32%). Anal. found: C, 31.61; H, 2.85; N, 4.68. Calcd: C, 31.70; H, 2.77; N, 4.62. Main IR frequencies (KBr, cm⁻¹): 3307, 3263, 3178, 1608, 1539, 1471, 1398, 898, 813, 779.

Preparation of Compound 2. A mixture of 5-aminoisophthalic acid (0.181 g, 1 mmol), Pr₆O₁₁ (0.150 g, 0.147 mmol), HNO₃ (3.00 mmol), and H₂O (10 mL) was heated to 150 °C for 50 h in a 23 mL Teflon-lined stainless-steel autoclave, and then it was cooled to room temperature at 10 °C h⁻¹ to obtain colorless platelike single crystals of **2** (yield: 5%). Anal. found: C, 26.53; H, 3.10; N, 6.38. Calcd: C, 26.46; H, 3.05; N, 6.43. Main IR frequencies (KBr, cm⁻¹): 3395, 3258, 3189, 2928, 1620, 1540, 1475, 1410, 950, 880, 815, 780.

- (2) (a) Rowsell, J. L. C.; Yaghi, O. M. *Microporous Mesoporous Mater.* **2004**, *73*, 3. (b) Kitagawa, S.; Kitaura, R.; Noro, S. *Angew. Chem., Int. Ed.* **2004**, *43*, 2334. (c) Rao, C. N. R.; Natarajan, S.; Vaidhy-anathan, R. *Angew. Chem., Int. Ed.* **2004**, *43*, 1466. (d) Mueller, U.; Schubert, M.; Teich, F.; Puetter, H.; Schierle-Arndt, K.; Pastre, J. J. *Mater. Chem.* **2006**, *16*, 626.
- (3) (a) Li, H.; Eddaoudi, M.; O'Keeffe, M.; Yaghi, O. M. *Nature (London)* **1999**, *402*, 276. (b) Seo, J. S.; Whang, D.; Lee, H.; Jun, S. I.; Oh, J.; Jeon, Y. J.; Kim, K. *Nature (London)* **2000**, *404*, 982. (c) Muller, A. *Science* **2003**, *300*, 749.
- (4) (a) Ding, B.-B.; Weng, Y.-Q.; Mao, Z.-W.; Lam, C.-K.; Chen, X.-M.; Ye, B.-H. *Inorg. Chem.* **2005**, *44*, 8836. (b) Pan, L.; Olson, D. H.; Ciemmolonski, L. R.; Heddy, R.; Li, J. *Angew. Chem., Int. Ed.* **2006**, *45*, 616. (c) Fang, Q.; Zhu, G.; Xue, M.; Sun, J.; Sun, F.; Qiu, S. *Inorg. Chem.* **2006**, *45*, 3582. (d) Becht, G.; Hwu, S.-J. *Chem. Mater.* **2006**, *18*, 4221.
- (5) (a) Markus, A. *Angew. Chem., Int. Ed.* **1999**, *38*, 3463. (b) Abrahams, B. F.; Batten, S. R.; Grannas, M. J.; Hamit, H.; Hoskins, B. F.; Robson, R. *Angew. Chem., Int. Ed.* **1999**, *38*, 1475. (c) Seidel, S. R.; Stang, P. J. *Acc. Chem. Res.* **2002**, *35*, 972. (d) Kumazawa, K.; Biradha, K.; Kusakawa, T.; Okano, T.; Fujita, M. *Angew. Chem., Int. Ed.* **2003**, *42*, 3909. (e) Behrens, E. A.; Poojary, D. M.; Clearfield, A. *Chem. Mater.* **1996**, *8*, 1236.
- (6) (a) Qiu, Y.; Liu, Z.; Li, Y.; Deng, H.; Zeng, R.; Zeller, M. *Inorg. Chem.* **2008**, *47*, 5122. (b) Deng, H.; Qiu, Y.; Daigebonne, C.; Kerbellec, N.; Guillou, O.; Zeller, M.; Batten, S. R. *Inorg. Chem.* **2008**, *47*, 5866. (c) Deng, H.; Qiu, Y. C.; Li, Y. H.; Liu, Z. H.; Zeng, R. H.; Zeller, M.; Batten, S. R. *Chem. Commun.* **2008**, 2239.
- (7) (a) Eddaoudi, M.; Kim, J.; Rosi, N.; Vodak, D.; Wachter, J.; O'Keeffe, M.; Yaghi, O. M. *Science* **2002**, *295*, 469. (b) Rosi, N. L.; Eckert, J.; Eddaoudi, M.; Vodak, D. T.; Kim, J.; O'Keeffe, M.; Yaghi, O. M. *Science* **2003**, *300*, 1127. (c) Rowsell, J. L. C.; Millward, A. R.; Park, K. S.; Yaghi, O. M. *J. Am. Chem. Soc.* **2004**, *126*, 5666. (d) Noro, S.; Kitagawa, S.; Kondo, M.; Seki, K. *Angew. Chem., Int. Ed.* **2000**, *39*, 2081.
- (8) (a) Tranchemontagne, D. J.; Ni, Z.; O'Keeffe, M.; Yaghi, O. M. *Angew. Chem., Int. Ed.* **2008**, *47*, 5136. (b) Ma, S.; Wang, X.-S.; Manis, E. S.; Collier, C. D.; Zhou, H.-C. *Inorg. Chem.* **2007**, *46*, 3432. (c) Ni, Z.; Yassar, A.; Antoun, T.; Yaghi, O. M. *J. Am. Chem. Soc.* **2005**, *127*, 12752. (d) Ma, B.-Q.; Zhang, D.-S.; Gao, S.; Jin, T.-Z.; Yan, C.-H.; Xu, G. X. *Angew. Chem., Int. Ed.* **2000**, *39*, 3644. (e) Hou, L.; Lin, Y.-Y.; Chen, X.-M. *Inorg. Chem.* **2008**, *47*, 1346.
- (9) (a) Humphrey, S. M.; Chang, J.-S.; Jhung, S. H.; Yoon, J. W.; Wood, P. T. *Angew. Chem., Int. Ed.* **2007**, *46*, 272. (b) Rosi, N. L.; Kim, J.; Eddaoudi, M.; Chen, B.; O'Keeffe, M.; Yaghi, O. M. *J. Am. Chem. Soc.* **2005**, *127*, 1504. (c) Xiao, D.-R.; Wang, E.-B.; An, H.-Y.; Su, Z.-M.; Li, Y.-G.; Gao, L.; Sun, C.-Y.; Xu, L. *Chem.—Eur. J.* **2005**, *11*, 6673.
- (10) (a) Jia, J.; Lin, X.; Blake, A. J.; Champness, N. R.; Hubberstey, P.; Shao, L.; Walker, G.; Wilson, C.; Schroll, M. *Inorg. Chem.* **2006**, *45*, 8838. (b) Serre, C.; Stock, N.; Bein, T.; Ferey, G. *Inorg. Chem.* **2004**, *43*, 3159. (c) Reineke, T. M.; Eddaoudi, M.; O'Keeffe, M.; Yaghi, O. M. *Angew. Chem., Int. Ed.* **1999**, *38*, 2590.
- (11) (a) Serre, C.; Millange, F.; Marrot, J.; Ferey, G. *Chem. Mater.* **2002**, *14*, 2409. (b) Zhang, L.-P.; Wan, Y.-H.; Jin, L.-P. *Polyhedron* **2003**, *22*, 981. (c) Wang, Y.; Zheng, X.; Zhuang, W.; Jin, L. *Eur. J. Inorg. Chem.* **2003**, 3572. (d) Zheng, X.-J.; Jin, L.-P.; Gao, S.; Lu, S.-Z. *Inorg. Chem. Commun.* **2005**, *8*, 72. (e) Daigebonne, C.; Guillou, O.; Gerault, Y.; Lecerf, A.; Boubekur, K. *Inorg. Chim. Acta* **1999**, *284*, 139.
- (12) (a) Wu, C.-D.; Lu, C.-Z.; Yang, W.-B.; Zhuang, H.-H.; Huang, J.-S. *Inorg. Chem.* **2002**, *41*, 3302. (b) Tang, E.; Dai, Y.-M.; Zhang, J.; Li, Z.-J.; Yao, Y.-G.; Zhang, J.; Huang, X.-D. *Inorg. Chem.* **2006**, *45*, 6276. (c) Tao, J.; Yin, X.; Jiang, Y.-B.; Huang, R.-B.; Zheng, L.-S. *Inorg. Chem. Commun.* **2003**, *6*, 1171. (d) Wu, C.-D.; Lu, C.-Z.; Zhuang, H.-H.; Huang, J.-S. *Z. Anorg. Allg. Chem.* **2002**, *628*, 1935. (e) Xiao, H.-P.; Li, X.-H.; Morsali, A.; Wang, J.-G.; Zhang, W.-B. *Z. Anorg. Allg. Chem.* **2007**, *633*, 1107. (f) Zhang, K.-L.; Qiao, N.; Gao, H.-Y.; Zhou, F.; Zhang, M. *Polyhedron* **2007**, *26*, 2461. (g) Banerjee, S.; Shanmugan, S.; Murugavel, R. *Struct. Chem.* **2007**, *18*, 165. (h) Aakeroy, J.; Desper, C. B.; Leonard, B.; Urbina, J. F. *Cryst. Growth Des.* **2005**, *5*, 865. (i) Kongshaug, K. O.; Fjellvag, H. *Inorg. Chem.* **2006**, *45*, 2424.

Table 1. Crystallographic Data and Structure Refinement Summary for Complexes **1** and **2**

| complex | 1 | 2 |
|---|--|--|
| formula | C ₂₄ H ₂₅ Pr ₂ N ₅ O ₁₇ | C ₂₄ H ₁₇ Pr ₂ N ₅ O ₁₈ |
| fw | 909.29 | 945.25 |
| cryst syst | triclinic | orthorhombic |
| space group | <i>P</i> $\bar{1}$ | <i>Pnma</i> |
| <i>a</i> (Å) | 8.8797(2) | 8.5785(4) |
| <i>b</i> (Å) | 10.4305(2) | 31.9322(15) |
| <i>c</i> (Å) | 16.8737(3) | 13.8236(7) |
| α (deg) | 84.383(1) | 90.0 |
| β (deg) | 79.454(1) | 90.0 |
| γ (deg) | 68.265(1) | 90.0 |
| <i>V</i> (Å ³) | 1426.43(5) | 3786(3) |
| <i>Z</i> | 2 | 4 |
| <i>D</i> _{calcd} (g/cm ³) | 2.117 | 1.658 |
| μ (mm ⁻¹) | 3.464 | 2.616 |
| <i>F</i> (000) | 888 | 1832 |
| params | 415 | 227 |
| goodness-of-fit (<i>F</i> ²) | 1.023 | 1.000 |
| <i>R</i> ₁ [<i>I</i> > 2 σ (<i>I</i>)] | 0.0424 | 0.0349 |
| <i>wR</i> ₂ (all data) | 0.1224 | 0.0901 |

Crystal Structure Determination. Single-crystal X-ray diffraction data collections of **1** and **2** were performed on a Bruker Apex II CCD diffractometer operating at 50 kV and 30 mA using Mo K α radiation ($\lambda = 0.71073$ Å). Data collection and reduction were performed using the APEX II software.¹³ Multiscan absorption corrections were applied for all of the data sets using the APEX II program.¹³ Both structures were solved by direct methods and refined by full-matrix least-squares on *F*² using the SHELXTL program package.¹³ All non-hydrogen atoms were refined with anisotropic displacement parameters. Hydrogen atoms attached to carbon were placed in geometrically idealized positions and refined using a riding model. Hydrogen atoms on water molecules or amino groups were located from difference Fourier maps and were also refined using a riding model. The SQUEEZE procedure was used to remove the highly disordered four water molecules hosted within the cavity of compound **2**, which was implemented in the molecular geometry program Platon.¹⁴ The *R* values improved from 0.0427 to 0.0349 and 0.1221 to 0.0901 for *R*₁ and *wR*₂, respectively, after application of the correction. Crystallographic data for **1** and **2** are presented in Table 1.

Results and Discussion

Hydro(solvo)thermal synthesis has significant advantages over other methods for the synthesis of coordination frameworks.¹⁵ In conjunction with this technique, lanthanide oxides were used as the lanthanide source so that the lanthanide ions were slowly released to lower the polymerization rate and lead to high-quality single crystals. Furthermore, in our previous work, perchloric acid and nitric acid were shown to play an important role in the construction of novel coordination frameworks.¹⁶

Single-crystal X-ray diffraction studies revealed that compounds **1** and **2** were open 3D coordination frameworks constructed by infinite rod-shaped praseodymium carboxylate

SBUs and phenyl links. As illustrated in Figure 1a, compound **1** crystallizes in the triclinic space group *P* $\bar{1}$ and has two crystallographically independent Pr(III) ions, three aip ligands, and two coordinated water molecules and three lattice water molecules per asymmetric unit. Both Pr(III) centers are eight-coordinated by seven carboxyl oxygen atoms from six aip ligands and one water molecule and can be described as having a bicapped trigonal prismatic geometry with Pr–O distances and O–Pr–O bond angles ranging from 2.358(5) Å to 2.773(5) Å and 48.82(15)° to 167.18(18)°, respectively. Whereas, compound **2** crystallizes in the orthorhombic space group *Pnma*, and it has one Pr(III) ion, one and a half aip ligands (one of which is protonated at the amine), one nitrate, and four lattice water molecules per asymmetric unit (Figure 1b). The Pr(III) center is nine-coordinated by nine oxygen atoms. Seven out of the nine are from carboxylate groups of six aip ligands, and the remaining two belong to one chelating nitrate group. The Pr–O distances and O–Pr–O bond angles range from 2.391(5) to 2.884(5) Å and 47.53(19)° to 156.61(19)°, respectively. This gives an overall distorted tricapped trigonal prismatic geometry around the metal center.

In the polymeric structure of **1**, the carboxylate groups of the three unique aip ligands adopt two different bridging modes (Figure 2a,b), resulting in the formation of a praseodymium–carboxylate chain along the *a* axis (Figure 2c). The infinite rod-shaped praseodymium–carboxylate chain can be regarded as a SBU, where the two unique praseodymium ions are separated by 4.238 (2) Å. These SBUs are sustained by rigid phenyl rings of aip ligands to construct a three-dimensional coordination framework (Figure 3a). The framework can be ideally regarded as interlinked infinite rod-shaped SBUs with small channels running along the *a* axis of the unit cell (Figure 3b). While assigning a definitive underlying network topology to this structure is difficult (the choice of which part of the 1D metal carboxylate chains to assign as a finite “node” is very subjective and somewhat arbitrary), Yaghi and co-workers have described a series of other metal carboxylate coordination polymers in terms of the packing and interconnection of 1D rods.^{9b} Under this nomenclature, compound **1** has a **pcu**-type rod packing. The channels in the framework host water molecules which are stabilized by H bonds involving –NH₂ groups and carboxylate groups. The size of the void created by the formal removal of the coordinated and uncoordinated water molecules is 207.5 Å³, which is 14.5% of the unit cell volume.¹⁴ In the polymeric structure of **2**, the carboxylate groups of the aip ligands again show two bridging modes (Figure 2a,b) and connect praseodymium centers to form infinite rod-shaped secondary building units (Figure 2d). The Pr–Pr distance is 4.496 (3) Å. The bridging backbones of the aip ligands then lead to the formation of an overall 3D structure with irregular large channels running along the *a* axis. The chelating NO₃ and uncoordinated amine and ammonium groups, good potential H-bonding donors and acceptors, point into the large channels (Figure 3c). The framework can also be rationalized as interlinked infinite rod-shaped SBUs (Figure 3d); the rod packing is of the **bnn** type.^{9b} The size

(13) APEXII, version 3.1.2; Bruker AXS Inc: Madison, WI, 2004. Sheldrick, G. M. *SHELXL-97*; University of Göttingen, Göttingen, Germany, 1997.

(14) Spek, A. L. *PLATON*; Utrecht University: Utrecht, The Netherlands, 2005.

(15) (a) Zhang, X.-M. *Coord. Chem. Rev.* **2005**, *249*, 1201. (b) Chen, X.-M.; Tong, M.-L. *Acc. Chem. Res.* **2007**, *40*, 162.

(16) Deng, H.; Qiu, Y.-C.; Li, Y.-H.; Liu, Z.-H.; Guillou, O. *Inorg. Chim. Acta* **2008**, in press. DOI: 10.1016/j.ica.2008.08.020.

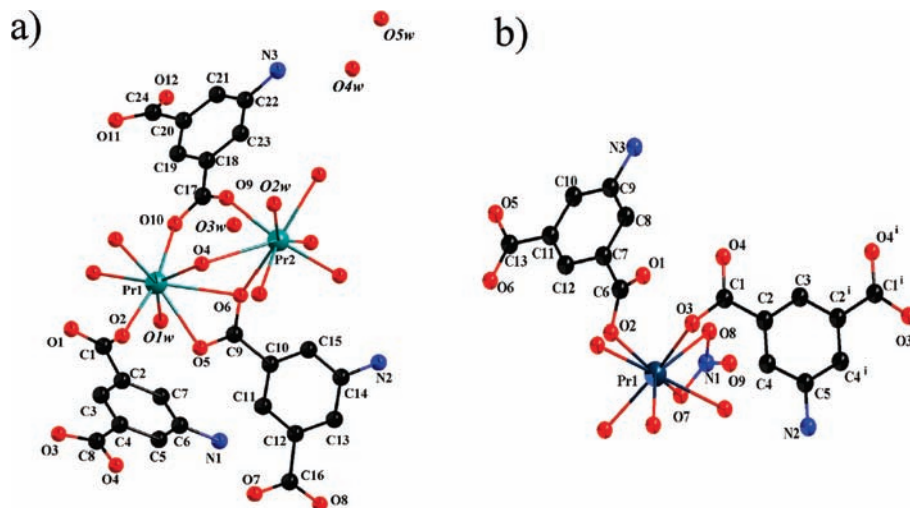


Figure 1. View of the asymmetric unit of structures **1** (a) and **2** (b). Symmetry code: (i) $x, 1.5 - y, z$. All H atoms were omitted for clarity.

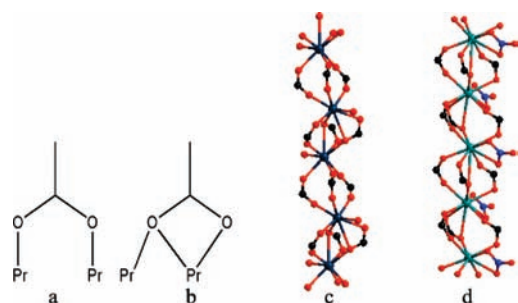


Figure 2. (a and b) Connection modes of carboxylate anions of aip ligands. (c and d) An infinite rod-shaped SBU of zigzag connection between adjacent Pr^{3+} centers in **1** and **2**, respectively.

of the void created by the formal removal of the free water molecules is 1069.6 \AA^3 , which is 28.2% of the unit cell volume.¹⁴

Properties. To determine the stability of the coordination polymers **1** and **2**, TGAs of **1** and **2** were performed under a nitrogen atmosphere. The TGA trace of compound **1** shows that the first weight loss of 6.09% from 80 to 120 °C corresponds to the loss of three guest molecules (calcd, 5.94%; see Figure S1, Supporting Information). Upon further heating, a second weight loss of 4.05% arises in the temperature range 210~230 °C (calcd 3.96%) and corresponds to the departure of coordination water molecules. Then, the aip ligands decompose, resulting in the collapse of the framework. The TGA trace of compound **2** shows that the intercalated water molecules are mainly removed in the temperature range 50~130 °C and that the resulting dehydrated nanoporous compound **2b** is stable up to 420 °C (found, 13.39%; calcd, 13.22%; see Figure S2, Supporting Information). The power X-ray diffraction of the guest-free phase $[\text{Pr}_2(\text{Haip})_2(\text{aip})(\text{NO}_3)_2]$ (**2b**) is almost identical to that of the as-synthesized **2** (Figure 4a,b). We have failed to get the structure redetermination of **2b**. Interestingly, the dehydrated powder of **2b** can be restored to the form of $\{\text{Pr}_2(\text{Haip})_2(\text{aip})(\text{NO}_3)_2 \cdot 8\text{H}_2\text{O}\}_n$ after being immersed in water for one day, as shown by the elemental analysis experiment (see Supporting Information) and power X-ray diffraction measurement results (Figure 4c,d). Moreover, as shown in Figure 4e and f, the stable channels of **2b** can also

reversibly host other small solvent molecules (e.g., methanol and ethanol), which are also determined by infrared spectra with the appearance of broad O–H and sharp C–H stretching vibrations in the region of 3400 and 2950 cm^{-1} , respectively.

Since, the dehydrated frameworks of **1** and **2** consist of 3D porous network structures, gas adsorption is the usual way to evaluate a material's porosity. Herein, we used a computational method to estimate the potential porosity of the dehydrated coordination polymers. In this context, we have formally partially dehydrated compounds **1b** and **2b**: The crystallization water molecules (easy to remove experimentally) are formally removed, while the coordination water molecules (strongly bonded to the metal ions) are not. The computational method, based on Connolly's algorithm,¹⁷ has already been described and successfully used elsewhere.^{6b,18} Thanks to it, the porosity profile of a partially dehydrated material can be designed on the basis of its crystal structure. As can be seen in Figure 5a, compound **1b** presents one type of channel spreading along the \bar{a} axis with a cavity radius of 1.2 Å, not big enough for being able to host molecules other than water molecules or He. However, compound **2b** exhibits large potential porosity. In order to compare the results of the calculations with experimental values, we have used a probe sphere presenting a radius of 1.8 Å, which is the usual kinetic radius of N_2 .^{9b} With this value, the potential specific accessible surface of this compound is 792 $\text{m}^2 \text{g}^{-1}$. Furthermore, as can be seen in the porosity profile (reported in Figure 5b), **2b** is able to host molecules with kinetic radii as big as 2.3 Å, which is in perfect agreement with what could be anticipated from the crystallographic data.

To get a better understanding of the porosity of **2b**, its sorption properties have been investigated using N_2 at 77 K. The N_2 gas sorption at 77 K shows a reversible type I

(17) Connolly, M. L. *Science* **1983**, *221*, 709.

(18) (a) Daiguebonne, C.; Kerbellec, N.; Bernot, K.; Gérault, Y.; Deluzet, A.; Guillou, O. *Inorg. Chem.* **2006**, *45*, 5399. (b) Guillou, O.; Daiguebonne, C.; Camara, M.; Kerbellec, N. *Inorg. Chem.* **2006**, *45*, 8468. (c) Qiu, Y.; Daiguebonne, C.; Liu, J.; Zeng, R.; Kerbellec, N.; Deng, H.; Guillou, O. *Inorg. Chim. Acta* **2007**, *360*, 3265.

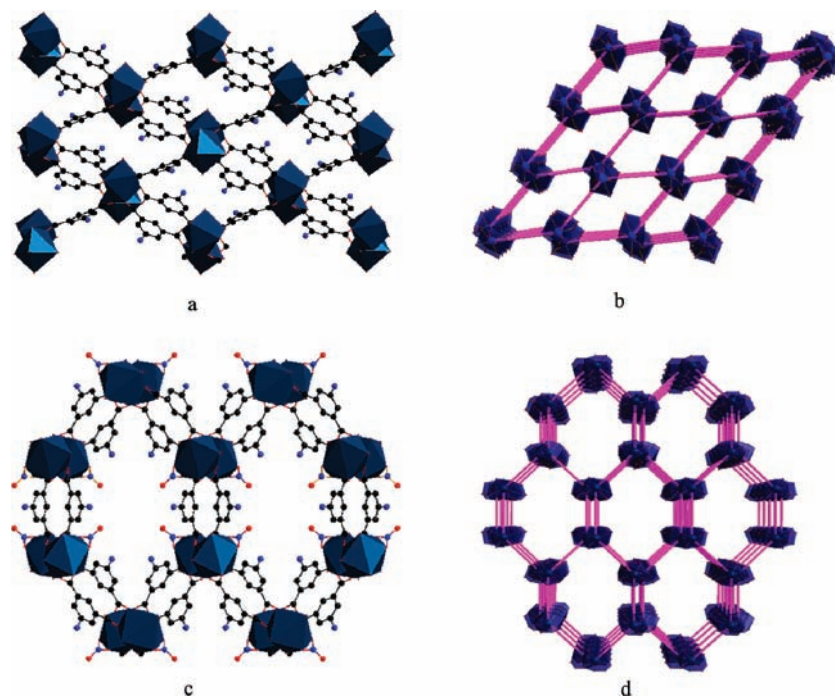


Figure 3. (a) View of channels in the a -axis direction and (b) schematic view of dehydrated compound **1**. (c) View of channels along the orthorhombic a -axis direction and (b) schematic view of dehydrated compound **2**. All hydrogen atoms are omitted for clarity.

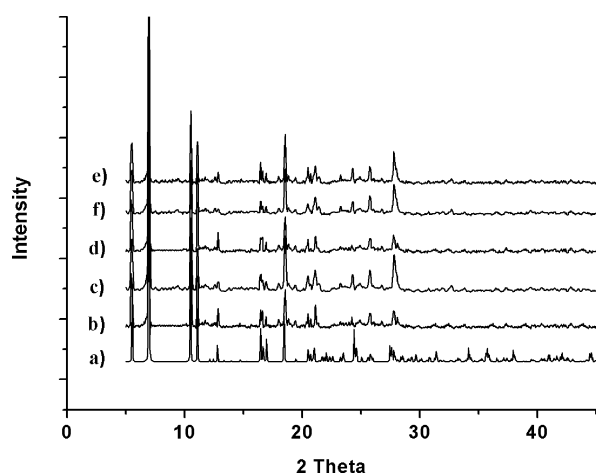


Figure 4. Powder X-ray diffraction patterns simulated from (a) the X-ray single-structure of **2**, (b) as-synthesized **2**, (c) hydrated compound **2b** $\{\text{Pr}_2(\text{Haip})_2(\text{aip})(\text{NO}_3)_2\}_n$, and (d) restored compound **2** and diffraction patterns obtained after being immersed in (e) methanol and (f) ethanol.

isotherm characteristic of microporous material¹⁹ (Figure 6) and calculated BET surface areas of 773 m^2/g . It has a slight deviation from the conventional type I isotherm at P/P_0 (0.08–0.6), suggesting the existence of a trace amount of mesoporous crystals, which are formed by agglomerating nanosized MOF crystallites. The N_2 uptake of 230 cm^3/g (STP; 287 mg/g) of **2b** is observed at 1 atm, which corresponds to 9.7 molecules per unit cell.

For the hydrogen adsorption behavior of **2b**, a GCMC simulation implemented by the sorption program in the MS modeling 4.0 package²⁰ was performed to predict its sorption

isotherm using standard algorithms. The structure of the unit cell was imported from compound **2b** and then fixed the simulation cell, consisting of $2 \times 1 \times 2$ unit cells. The cutoff radius was set to 12.5 Å. The simulations were carried out at a temperature of 77 K and in the pressure range 0–100 kPa. For each state point, the GCMC simulation consisted of 2×10^6 steps to guarantee equilibration, followed by 2×10^6 steps to sample the desired thermodynamic properties. The program for GCMC simulations of the adsorption of fluids in porous materials has been verified in previous reports.²¹ For the hydrogen molecules, the two-site Lennard-Jones potential model suggested by Yang and Zhong^{21a,b} was adopted. For the structural modeling, the procedure was based on the standard universal force field²¹ with some refined parameters, which has successfully been used to study the adsorption isotherms of a series of IRMOFs.^{21–23} Whereas, GCMC simulation studies on hydrogen storage in MOFs based on infinite rod-shaped SBUs are very scarce. Herein, we performed molecular simulations of hydrogen sorption in two MOFs analogous to our MOF-**2b** in advance, as shown in Figure S3, Supporting Information; the simulation results are in reasonable agreement with the experimental data for $\text{Ln}_2(\text{PDC})_3$ ($M = \text{Y}, \text{Er}$; $\text{PDC} = \text{pyridine-3,5-dicarboxylate}$) at 77 K and 1 atm.^{10a} For the structure of **2b**, a similar simulated adsorption isotherm is shown in Figure S4 (Supporting Information); we found that **2b** can absorb

(21) (a) Yang, Q.; Zhong, C. *J. Phys. Chem. B* **2005**, *109*, 11862. (b) Yang, Q.; Zhong, C. *J. Phys. Chem. B* **2006**, *110*, 655. (c) Jung, D. H.; Kim, D.; Lee, Tae, B. S.; Choi, B.; Yoon, J. H.; Kim, J.; Choi, K.; Choi, S.-H. *J. Phys. Chem. B* **2006**, *110*, 22987.

(22) (a) Rappe, A. K.; Casewit, C. J.; Colwell, K. S.; Goddard, W. A., III. *J. Am. Chem. Soc.* **1992**, *114*, 10024. (b) Castonguay, L. A.; Rappe, A. K. *J. Am. Chem. Soc.* **1992**, *114*, 5832.

(23) (a) Vishnyakov, A.; Ravikovitch, P. I.; Neimark, A. V.; Bulow, M.; Wang, Q. M. *Nano Lett.* **2003**, *3*, 713. (b) Düren, T.; Sarkisov, L.; Yaghi, O. M.; Snurr, R. Q. *Langmuir* **2004**, *20*, 2683.

(19) Gregg, S. J.; Sing, K. S. W. *Adsorption, Surface Area and Porosity*; 2nd ed.; Academic Press: London, U.K., 1982.

(20) *Materials Studio Getting Started*, release 4.0; Accelrys Software, Inc.: San Diego, CA, 2006.

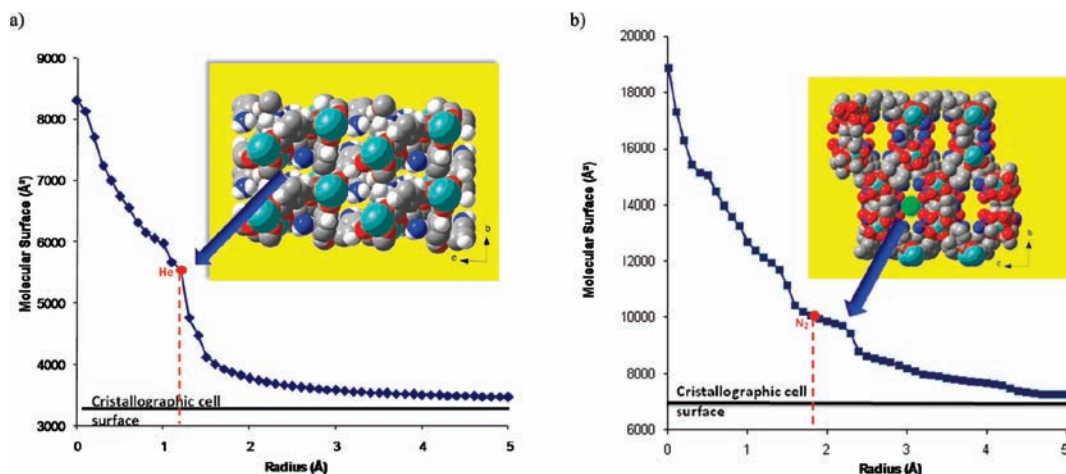


Figure 5. (a and b) Porosity profile (molecular surface versus probe sphere radius) for compounds **1** and **2**, respectively.

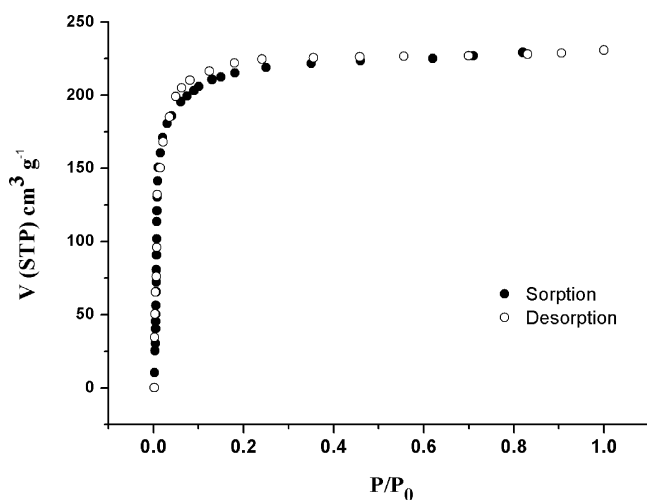


Figure 6. N₂ adsorption isotherms (77 K) for **2b**.

4.7 mg of H₂ per gram at 77 K and 1 atm, that is, 2.2 H₂ per formula unit of compound **2b**. The hydrogen capacity can be clearly explained via the snapshots of the structures of **2b** with adsorbed hydrogen molecules at various pressures (see Figure S5, Supporting Information). Initially, hydrogen molecules locate the corner regions between nitrate and amino groups close to rod-shaped praseodymium–carboxylate units, and then the aromatic units start adsorbing hydrogen molecules at higher pressures, followed by the filling of the inner spaces of the cavities. This is in accordance with the

experimental observations of Rosi et al.^{7b} and Kubota et al.,²⁴ who deduced that hydrogen molecules prefer to be absorbed close to metal–oxygen units. Therefore, the amino groups in the adsorption of hydrogen molecules within the cavities should be advantageous when designing new materials.

In summary, two new 3D praseodymium coordination frameworks with different porosities have been prepared under hydrothermal conditions on the basis of different acids. The porosities of both dehydrated coordination frameworks were estimated using a computational method based on Connolly's algorithm, showing that **2b** has a significant potential specific accessible surface, high N₂ storage based on BET experiments, and good hydrogen absorption capacity at 77 K and 1 atm on the basis of grand canonical Monte Carlo simulation. Furthermore, powder X-ray diffraction measurement results demonstrated that the stable channels of **2b** can reversibly host other small solvent molecules (e.g., water, methanol, and ethanol).

Acknowledgment. This work was supported by National Natural Science Foundation of China, Grant No. 20871048.

Supporting Information Available: X-ray crystallographic files (CIF) for **1** and **2**, TGA traces, GCMC simulation isotherm. This material is available free of charge via the Internet at <http://pubs.acs.org>.

IC8020518

(24) Kubota, Y.; Takata, M.; Matsuda, R.; Kitaura, R.; Kitagawa, S.; Kato, K.; Sakata, M.; Kobayashi, T. C. *Angew. Chem., Int. Ed.* **2005**, *44*, 920.